# Comparison of wavelength dependence in cascade-, Λ-, and Vee-type schemes for electromagnetically induced transparency

J. R. Boon, E. Zekou, D. McGloin, and M. H. Dunn
*J. F. Allen Physics Research Laboratories, Department of Physics and Astronomy, University of St. Andrews, North Haugh, St. Andrews, Fife KY16 9SS, Scotland, United Kingdom*

(Received 15 June 1998; revised manuscript received 2 September 1998)

We present a theoretical study of the effects of mismatching wavelengths for the coupling and probe fields in Doppler-broadened media for the three basic energy level configurations commonly used to realize electromagnetically induced transparency (EIT). Three wavelength regimes are considered: mismatched wavelengths for which the coupling frequency is greater than the probe frequency, matched wavelengths for which the coupling and probe frequencies are equal, and mismatched wavelengths for which the probe frequency is greater than the coupling frequency. The transparency that may be induced in these regimes is compared for the cascade-, Λ-, and Vee-type systems. We show that in the first mismatched regime ($\lambda_c<\lambda_p$) EIT is possible in all schemes and is in fact stronger than in the matched case. It is also demonstrated that for the second mismatched regime ($\lambda_c>\lambda_p$) EIT can be realized most readily in the Vee-type configuration in the presence of Doppler broadening. These predictions are explained by considering the absorption as a function of both the probe field detuning and the atomic velocity. [S1050-2947(99)01006-9]

PACS number(s): 42.50.Gy, 42.50.Hz, 32.80.Qk, 32.60.+i

## I. INTRODUCTION

Amplification and lasing without inversion has recently been the subject of much experimental work [1–14]. This research culminated in the first observation of continuous wave (cw) inversionless lasing by Zibrov and co-workers in 1995 [10]. The Zibrov scheme utilized matched (equal probe and coupling frequency) wavelengths in a gaseous medium subject to the effects of Doppler broadening. While it has been thought that mismatched (unequal probe and coupling frequencies) wavelength systems subject to Doppler broadening can only be realized for high coupling field powers [15], such mismatched schemes will be necessary to achieve the goal of high-frequency inversionless laser systems. Indeed, the impetus for studying lasing in the absence of inversion is to create lasing on problematic high-frequency transitions that cannot be accessed by conventional means due to the requirement of a population inversion. Now that the principle of lasing without inversion (LWI) has been demonstrated, it is pertinent to consider regimes for which the employed optical fields are unequal in wavelength. In this context, we study the phenomenon of electromagnetically induced transparency (EIT) [16–18] that creates the underlying reduction in absorption upon which LWI is based.

The consequences of mismatching the probe and coupling wavelengths on the transparency induced in the cascade-, Λ-, and Vee-type schemes are considered. The limitations imposed by Doppler broadening are explored and we explain the surprising discovery that EIT is still realizable for mismatched wavelengths in all three schemes, and particularly for probe frequencies higher than the employed coupling frequency in the Vee-type system. This is an important result for the study of EIT and lasing without inversion and is explained in terms of the ''many pathways to absorption'' description of EIT, considering the absorption as a function of atomic velocity as well as probe field detuning. We explore how mismatching the wavelengths in each scheme affects the position of the Autler-Townes components and the single- and two-photon absorption resonances. These are the determining factors in EIT, along with the magnitude of the Autler-Townes components as a function of frequency.

Previous work characterizing the effects of Doppler broadening has shown that matching the probe and coupling frequencies [19] allows the EIT feature to be resolved despite such effects, and that this is dependent on selecting the proper geometry of either copropagating or counterpropagating beams [20]. Our analysis concurs with these earlier studies and extends to the case of EIT realized with mismatched wavelengths.

In earlier papers we have shown both experimentally and theoretically that EIT is more pronounced in cascade systems for which the coupling frequency is greater than the probe frequency than for a matched cascade scheme [21], and that EIT is possible in a Vee-type Doppler-broadened scheme for probe frequencies greater than the coupling frequency [22]. This paper widens the study to include all three possible energy level configurations for EIT and both directions of relative wavelength mismatch.

## II. BASIS OF COMPARISON

A valid comparison of the wavelength dependence in the three EIT schemes is impossible without creating hypothetical energy level structures. In this way a comparison can be made solely on the basis of the type of scheme and the relative mismatch of the probe and coupling wavelengths, while all other parameters are kept constant. This would not be possible if we based the study on real atomic systems. A comparison of real cascade-, Λ-, and Vee-type schemes has previously been carried out by Fulton *et al.* [23], but only for the case of closely matched wavelengths.

Here we assume closed three level systems as shown in

 ©1999 The American Physical Society

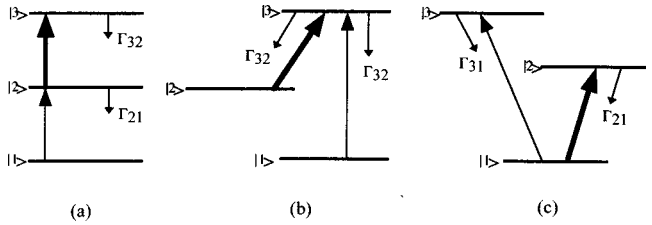


FIG. 1. Energy level configurations of (a) the cascade, (b) the Λ, and (c) the Vee-type schemes employed in the theoretical comparison presented in this paper.

Fig. 1 for (a) the cascade-, (b) the Λ-, and (c) the Vee-type configurations. All the decay rates, shown in Fig. 1, are set to $40\times10^6\,s^{-1}$ and the dephasing on the unlinked transition is also set to $40\times10^6\,s^{-1}$ for every system. The latter value corresponds to the maximum dephasing that would naturally occur due to level lifetime effects alone given the selected decay rates.

In order to directly compare all the absorption profiles the wavelength of the probe transition is kept constant while three values are selected for the coupling field. The probe wavelength was taken to be 800 nm with three coupling wavelengths of 400, 800, and 1600 nm. This leads to a total of nine considered systems; i.e., three wavelengths regimes ($\lambda_c<\lambda_p$, $\lambda_c=\lambda_p$, and $\lambda_c>\lambda_p$) for each of the three energy level schemes. We ensure that the chosen probe Rabi frequency, 100 kHz, does not significantly populate the upper level of the probe transition and choose a coupling field Rabi frequency that is approximately half the Doppler width; these values are 250 and 500 MHz, respectively. The Doppler width is based on rubidium at a temperature of 40 °C, for which significant absorption on the infrared rubidium transitions occurs ($80\ m^{-1}$). Rubidium vapor has been utilized in a wide range of EIT amplification and lasing without inversion experiments [6,7,9,10].

The analysis of these systems is carried out utilizing the semiclassical density-matrix formalism [24]. The equations describing the slowly varying density-matrix components have been described by ourselves [25], and other authors [26,27], along with the methods employed to solve them.

## III. THEORETICAL RESULTS

The calculated absorption profiles predicted for each system are presented in Fig. 2. Figures 3, 4, and 5 provide two-dimensional displays of the Autler-Townes absorption components and the single- and two-photon absorption resonance positions as a function of probe field detuning and atomic velocity for the different schemes. The explanation of our results relies on the fact that the change in absorption with atomic velocity is different in each of the three schemes and for each of the wavelength regimes. In Figs. 3, 4, and 5, we follow a similar display technique to that taken by Townes and Schawlow [28], in that we plot, as a function of probe field detuning, the individual contributions made by the different velocity groups across the Doppler profile make to the absorption of the probe in the presence of the coupling field. A horizontal line taken across the diagram refers to a particular velocity group. The points at which such an horizontal line intersects the two plotted curves gives the probe

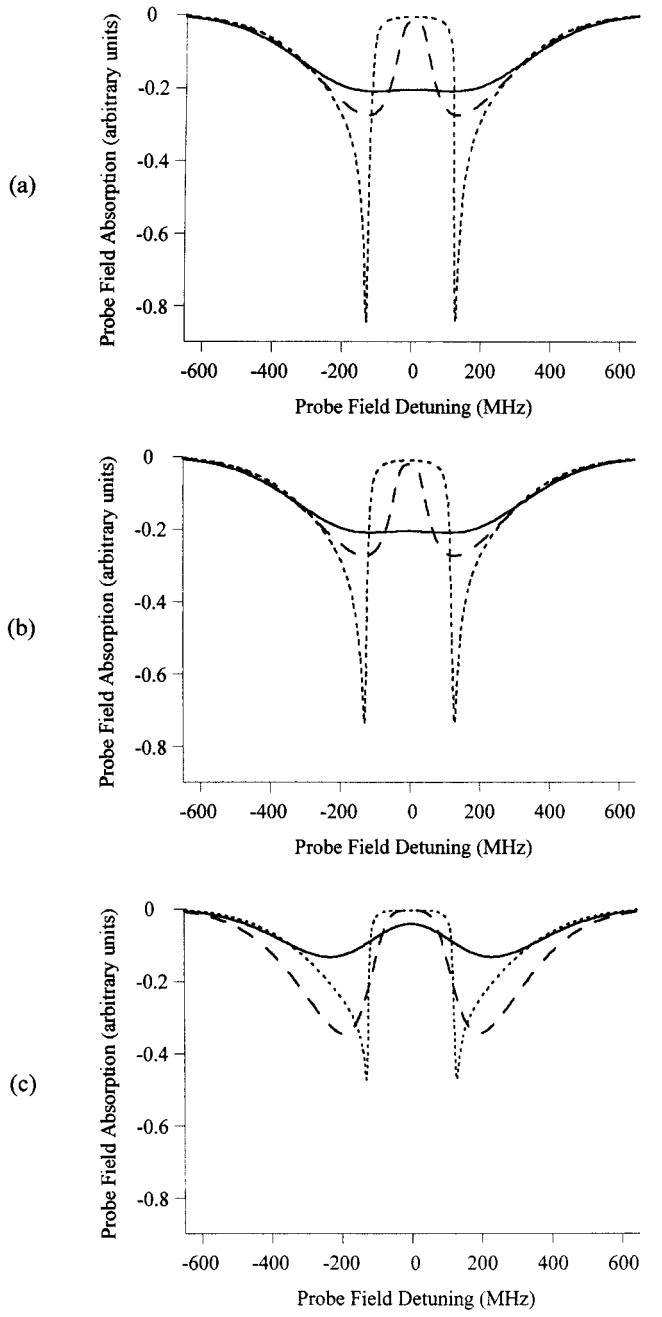


FIG. 2. Probe field absorption as a function of probe field detuning for (a) the cascade, (b) the Λ, and (c) the Vee-type schemes. In each case the three wavelength regimes are considered: $\lambda_c<\lambda_p$ (dotted line), $\lambda_c=\lambda_p$ (dashed line), and $\lambda_c>\lambda_p$ (solid line). For ease of comparison the same vertical scale is used in (a), (b), and (c).

field detunings corresponding to the locations of the Autler-Townes components for that particular velocity group. The thickness of the plotted curve at each point of intersection gives the absorption associated with that particular Autler-Townes component as experienced by the probe field. The absorption is calculated using a density-matrix analysis, with due allowance being made for the relative population of atoms in the particular velocity group as well as for the effects of detuning. It is important to note that the thickness should be read along a normal to the tangent at the given point on the curve. This avoids ambiguities at the turning point on

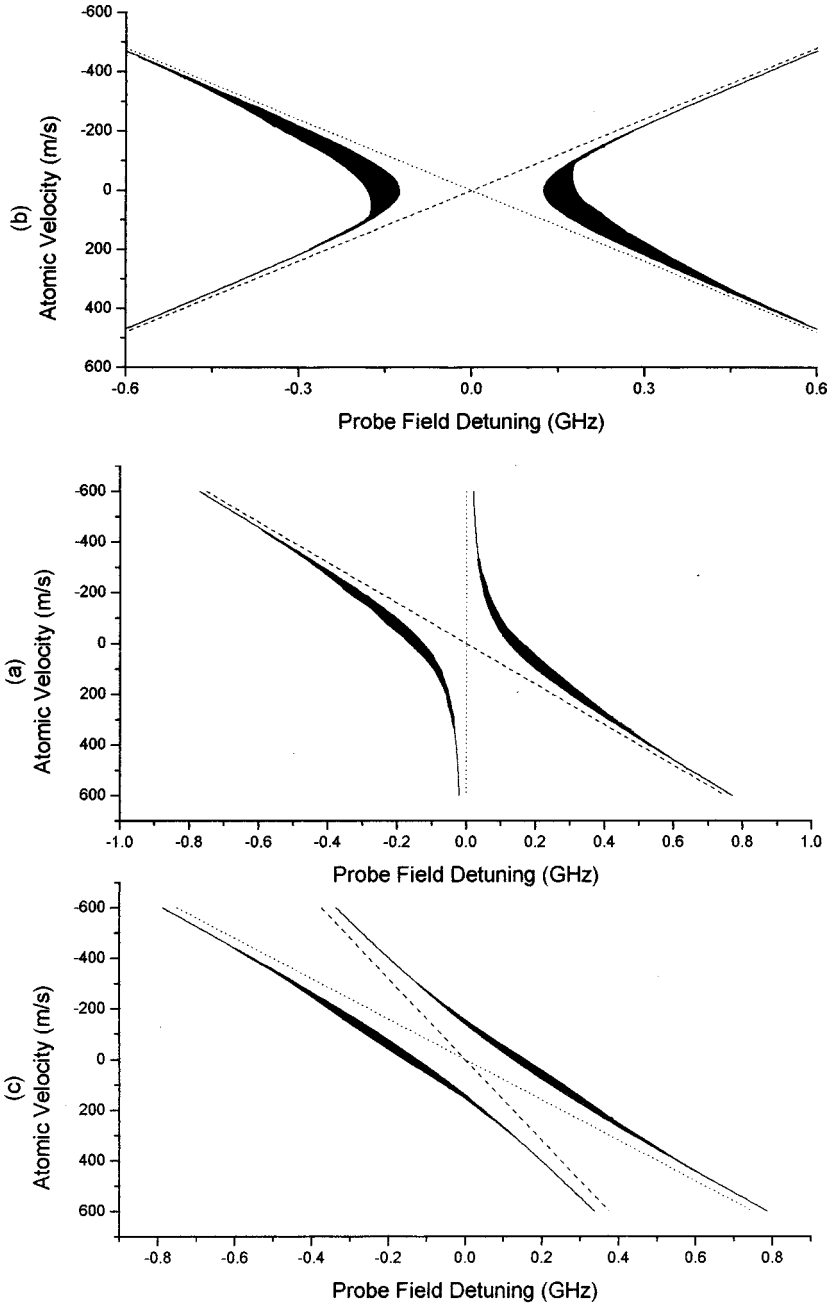


FIG. 3. Plots of the Autler-Townes and absorption resonance positions as a function of atomic velocity and probe field detuning for the cascade scheme. Three wavelengths regimes are considered: (a) $\lambda_c < \lambda_p$, (b) $\lambda_c = \lambda_p$, and (c) $\lambda_c > \lambda_p$. The magnitude of the Autler-Townes components is indicated, in each plot, by the thickness of the lines read in the direction of the normal to the tangent to the Autler-Townes components at a given atomic velocity. The thickness of these lines is proportional to the absorption coefficient for the atomic velocity specified. The positions of the Autler-Townes components are shown by solid lines, the single photon resonance by a dashed line, and the two-photon resonance by a dotted line.

some of the curves. If a vertical line is drawn on the diagram corresponding to a particular probe field detuning, the locations of its intersection(s) with the plotted curves identify the velocity group or groups (predominantly) responsible for the absorption experienced by the probe field. Further, the sum of the thicknesses of the two curves at these intersection points indicate the total absorption experienced by the probe field at such a detuning. These plots thus contain all the information necessary to explain the presence or lack of a transparency in the associated absorption profile.

In calculating the curves, we assume copropagating beams in the $\Lambda$- and Vee-type schemes and counterpropagating beams in the cascade scheme. By selecting these beam geometries, differences in the nature of the energy level configurations are counterbalanced, so that the Autler-Townes components and absorption resonances occur in the same positions for all three schemes, for a given set of probe and coupling wavelengths. In other words when we examine the zero velocity group the Autler-Townes components are symmetrical about the zero detuning point. When the coupling field is detuned, however, the components become asymmetric. By choosing the appropriate beam geometries we ensure that the locations of the two components for a given velocity group are the same in each of the schemes for a given ratio of probe and coupling field wavelength. It is *only* the magnitudes of the absorption that change between the three schemes in each of the wavelength regimes.

In the discussion that follows we distinguish two types of Autler-Townes components for any given system by noting that for high velocities the components split further apart and one follows the position of the single-photon resonance while the other follows the two-photon resonance. We refer

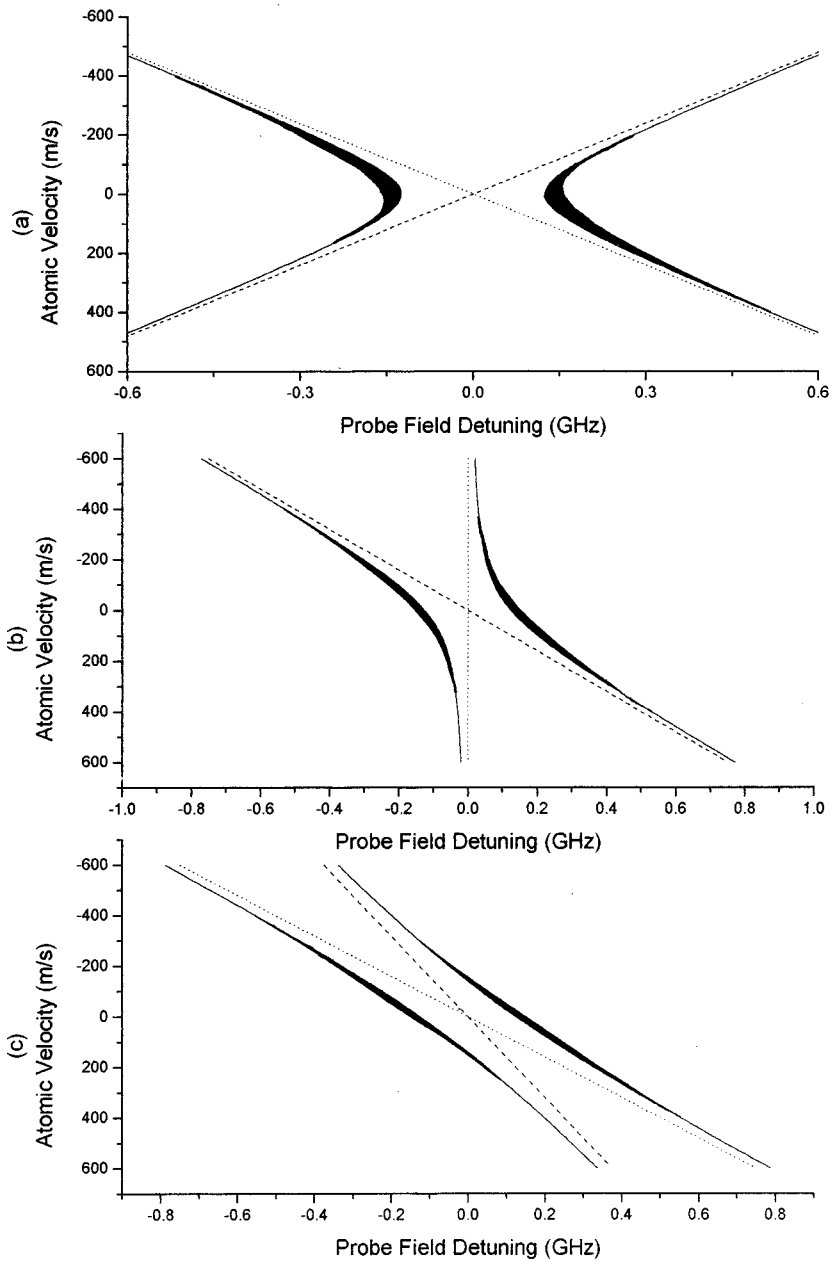


FIG. 4. Plots of the Autler-Townes and absorption resonance positions as a function of atomic velocity and probe field detuning for the $\Lambda$ scheme. Three wavelengths regimes are considered: (a) $\lambda_c<\lambda_p$, (b) $\lambda_c=\lambda_p$, and (c) $\lambda_c>\lambda_p$. The magnitude of the Autler-Townes components is indicated, in each plot, by the thickness of the lines read in the direction of the normal to the tangent to the Autler-Townes components at a given atomic velocity. The thickness of these lines is proportional to the absorption coefficient for the atomic velocity specified. The positions of the Autler-Townes components are shown by solid lines, the single photon resonance by a dashed line, and the two-photon resonance by a dotted line.

to the former as the primary Autler-Townes component and the latter as the secondary Autler-Townes component. As an illustration the primary and secondary Autler-Townes components are labeled in Fig. 6 for the matched wavelength case.

## IV. DISCUSSION

By considering the absorption profiles in Fig. 2 we can immediately see that the matched wavelength regime does not provide the best transparency in any of the energy level schemes. In fact, the highest level of transparency is induced in the mismatched wavelength regime for which the coupling frequency is higher than the probe frequency ($\lambda_c<\lambda_p$).

In a vee-type scheme we can think of EIT occurring due to the interference of two pathways to absorption in the bare-state picture [6,29]. Absorption of a single photon may occur exciting an atom from state $|1\rangle$ to state $|2\rangle$, or involving two photons—one from each field—stimulating the atom from state $|3\rangle$ to state $|1\rangle$ and then to state $|2\rangle$ as shown in Fig. 7. By considering the positions of the single- and two-photon absorption resonances in Figs. 3, 4, and 5 we see that the resonances for the two pathways to absorption are only coincident, for all schemes regardless of the probe and coupling field wavelengths, for zero atomic velocity. However, the absorption processes associated with a particular velocity group are not confined to a single discrete frequency but extend over a frequency range, which is the homogeneously broadened line-shape function centered on the positions indicated in Figs. 3, 4, and 5. Interference, and hence EIT, may therefore occur at any point for which the single- and two-photon absorption line shapes overlap to this extent. For the case in which the magnitudes of the absorption routes are equal, for a specific frequency, full cancellation may take place. When the magnitudes of the absorptions at a specific frequency are unequal, a partial reduction in absorption will

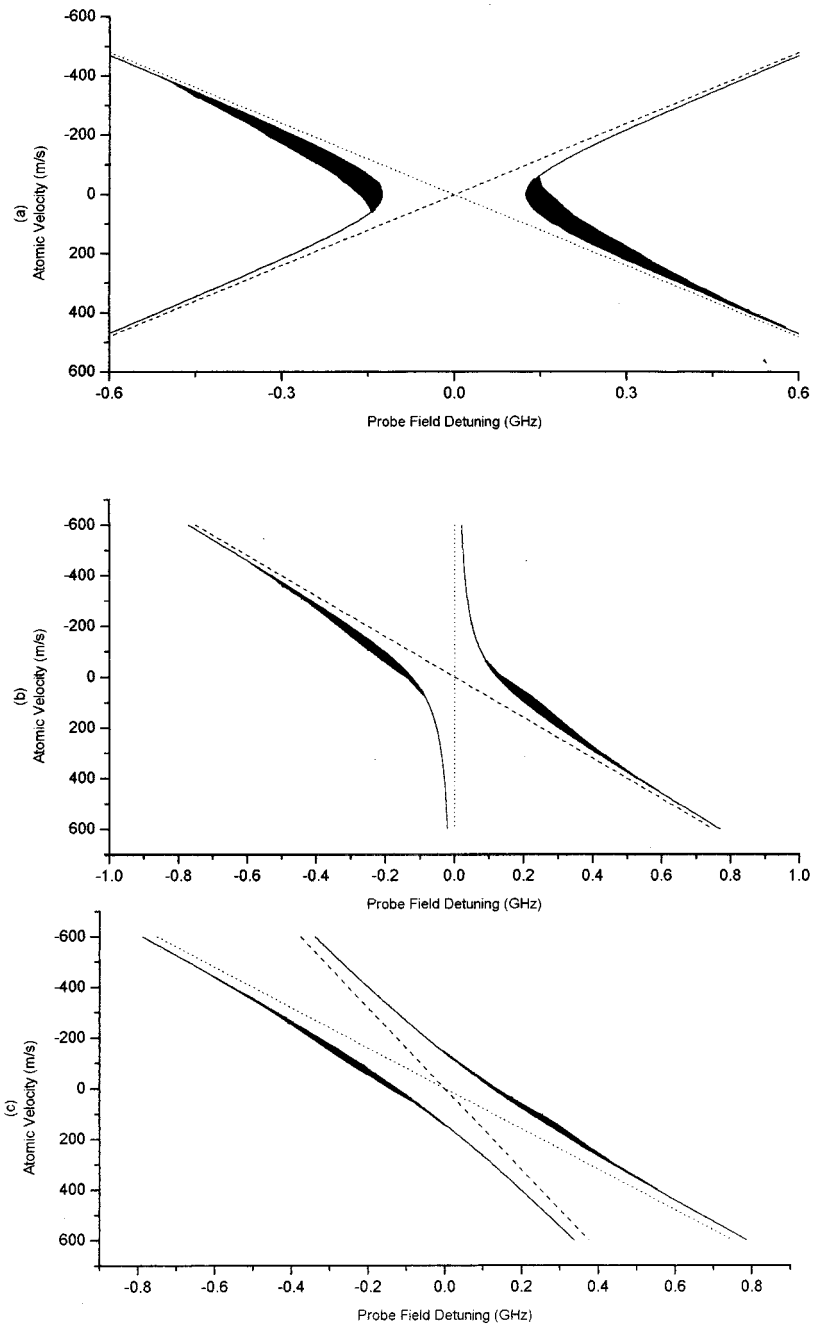


FIG. 5. Plots of the Autler-Townes and absorption resonance positions as a function of atomic velocity and probe field detuning for the Vee-type scheme. Three wavelengths regimes are considered: (a) $\lambda_c<\lambda_p$, (b) $\lambda_c=\lambda_p$, and (c) $\lambda_c>\lambda_p$. The magnitude of the Autler-Townes components is indicated, in each plot, by the thickness of the lines read in the direction of the normal to the tangent to the Autler-Townes components at a given atomic velocity. The thickness of these lines is proportional to the absorption coefficient for the atomic velocity specified. The positions of the Autler-Townes components are shown by solid lines, the single photon resonance by a dashed line, and the two-photon resonance by a dotted line.

occur. If, on the other hand, the absorption resonances for a given velocity are separated by much more than one homogeneous linewidth EIT does not take place, and it becomes important to ensure that the associated (Autler-Townes split) absorption components do not obscure the transparency that is created on resonance for other velocity groups.

The best transparency occurs when the coupling frequency is higher than the probe frequency because the Doppler-shifted contribution to the coupling field detuning, referred to here as the Doppler detuning, is greatest in this case. The Doppler shift in the frequency of the coupling field is proportional to the frequency of the coupling field itself and will, therefore, increase in magnitude when we decrease the coupling field wavelength. Consequently, Autler-Townes splitting, which is dependent on detuning, will also increase as the coupling wavelength decreases. In the $\lambda_c<\lambda_p$ regime the Autler-Townes components for the nonzero velocity atoms are split further apart and, therefore, further away from resonance. Thus, EIT created at line center for the zero velocity group is better preserved in this mismatched wavelength regime because the Autler-Townes components of the nonzero velocity atoms are Doppler detuned away from resonance and do not overlap with the transparency. Part (a) of Figs. 3, 4, and 5 clearly show the Autler-Townes splitting increasing with the modulus of the velocity so that coincidence of the single- and two-photon resonances (the point for which maximum EIT occurs) at line center is unobscured.

As we increase the coupling wavelength relative to the probe wavelength the magnitude of the Doppler detuning decreases relative to the Doppler width of the absorption profile, which is fixed by the probe wavelength. The Autler-Townes splitting for the nonzero velocity atoms will tend

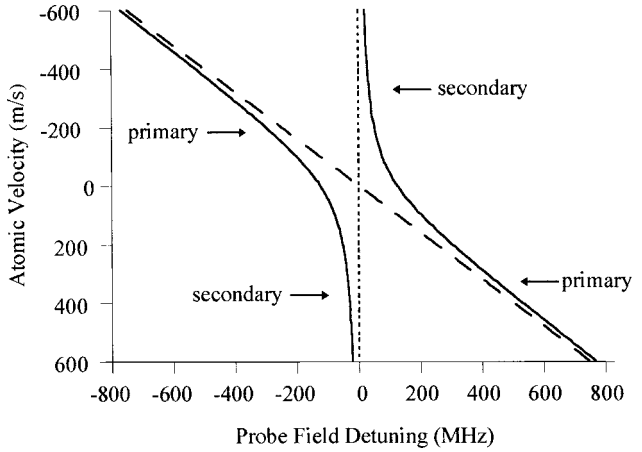


FIG. 6. Plot of the Autler-Townes and absorption resonance positions as a function of atomic velocity and probe field detuning in the matched wavelength case. The primary and secondary Autler-Townes components are clearly labeled.

towards that for the zero velocity atoms and the associated Autler-Townes absorptions will start to overlap with the line center transparency. The matched wavelength regime represents the special case when the Doppler shifts of the probe and coupling fields are equal and exactly cancel, ensuring that the two-photon resonance position is fixed for all velocity groups. The result is that the nonzero velocity, secondary, Autler-Townes absorptions only partially obscure the on-resonance transparency. The extent to which the transparency can be maintained in this regime depends largely on the dephasing. If dephasing is increased the linewidth of the Autler-Townes absorption components close to resonance will increase and further encroach on the transparency window.

In the $\lambda_c > \lambda_p$ regime Figs. 3(c), 4(c), and 5(c) show that the Autler-Townes components overlap completely with line center. We would reasonably expect the transparency created on resonance to be obscured and this is exactly what happens in the $\Lambda$ and cascade systems. However, in the Vee-type scheme the transparency window is maintained to a greater extent. This can be explained by considering the magnitude of the Autler-Townes components close to resonance. Careful inspection of the traces depicted in Figs. 3, 4, and 5 reveals that while the positions of the Autler-Townes components are the same in each energy-level scheme, for a given set of wavelengths, the magnitudes are different. For high, positive and negative velocities the primary and secondary Autler-Townes components separate and closely follow the single- and two-photon resonance positions. In this regime the magnitudes of each component is determined predominantly by the particular absorption resonance associated with it. The single-photon absorption defines the magnitude of the primary Autler-Townes component and the two-photon absorption determines the magnitude of the secondary component. It is the secondary Autler-Townes components that overlap with the on-resonance transparency in the $\lambda_c > \lambda_p$ regime. In a Vee-type system the magnitude of these secondary components falls off very rapidly as velocity increases and consequently the transparency at line center is not destroyed to the same extent as it is in the cascade and $\Lambda$ schemes.

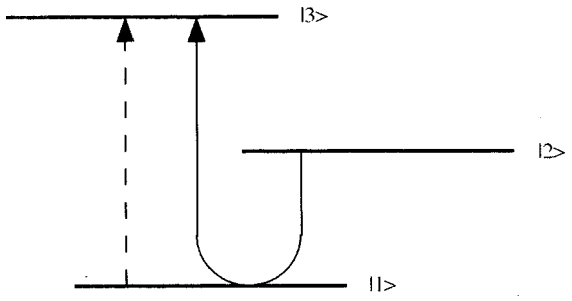


FIG. 7. The one- and two-photon routes in a Vee scheme. It is interference between these routes that leads to EIT.

In all three schemes it is also apparent that the magnitudes of these secondary Autler-Townes components fall off more rapidly with increasing velocity when the coupling wavelength is lower. This trend occurs because, as has been pointed out above, the Doppler-shifted contribution to the coupling field detuning, for a given velocity, is greater for a higher coupling field frequency. Consequently, the coupling field detuning changes and the two-photon resonance moves further from the intermediate atomic level as the coupling field wavelength is decreased. Since the magnitude of the secondary Autler-Townes components are dependent on the strength of the two-photon process they reduce as the two-photon resonance moves away from simultaneous resonance with the intermediate state. This diminution of the secondary Autler-Townes components always occurs as velocity increases in a given system. Importantly, it occurs more rapidly when coupling wavelength is lower and the Doppler shift is consequently greater for a given velocity.

The preceding argument applies to all three considered schemes but the Vee configuration exhibits a more sudden reduction in the magnitude of the secondary Autler-Townes components. The explanation for this lies in the nature of the two-photon process. In a Vee scheme the two-photon absorption route begins in the upper level of the coupling transition and, therefore, relies on that level being significantly populated. When the coupling field is detuned by the Doppler shift associated with nonzero velocity atoms, the population excited into the upper level of the coupling transition rapidly falls off. Consequently, the reduction in the magnitude of the two-photon absorption is markedly more rapid in a Vee scheme with increasing atomic velocity and the secondary Autler-Townes components that overlap with line center are of such a low magnitude that the transparency may still be observed.

To demonstrate the difference in the nature of the two-photon process in each scheme we consider the situation for which the coupling laser is scanned in frequency away from resonance with the $|1\rangle$-$|2\rangle$ transition. Figure 8 shows a series of traces, for each energy level scheme, in which the coupling field is manually detuned. EIT diminishes as the manual detuning of the coupling laser is increased because the two-photon and single-photon resonances no longer coincide at line center. Gradually the single and two-photon processes are resolved as distinct absorption peaks. However, the isolated two-photon absorption peak quickly disappears with increasing detuning in the Vee scheme while it persists for the $\Lambda$ and cascade systems.

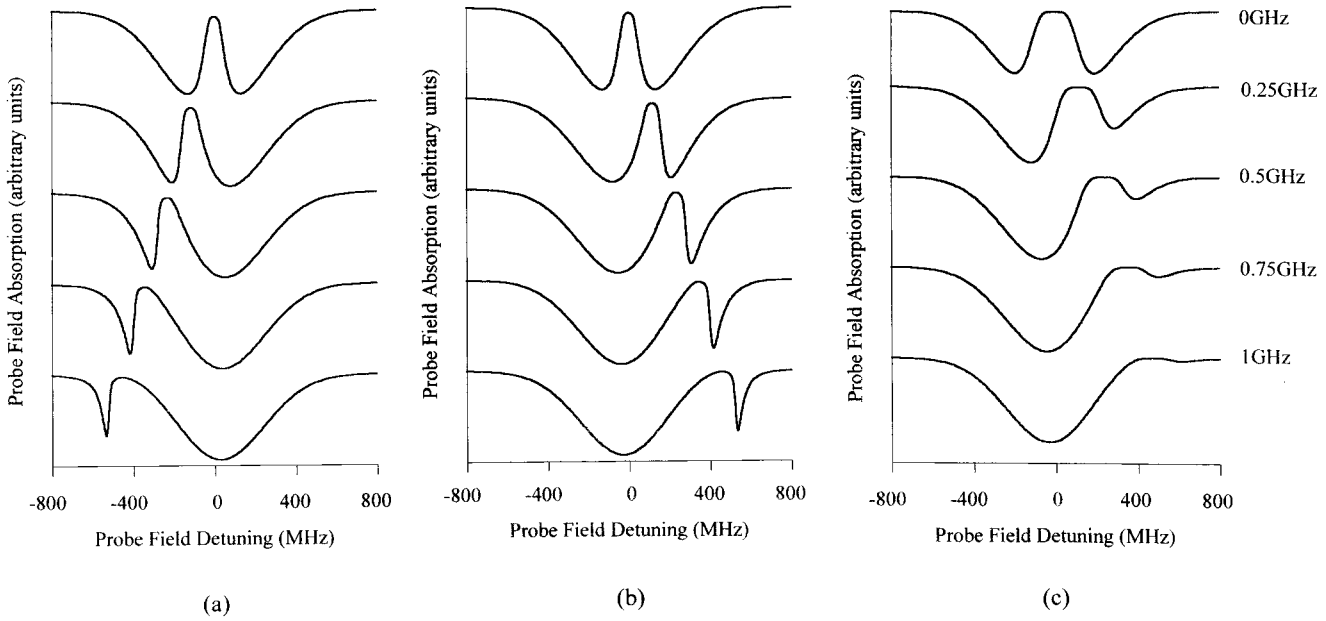


FIG. 8. A series of absorption profiles showing manual detuning of the coupling field in (a) the cascade, (b) the Λ, and (c) the Vee-type systems. The coupling field detuning associated with each trace is indicated to the right of the figure. The topmost trace shows the single and two-photon absorption routes interfering to create EIT and the bottom trace shows the resolved absorption profiles of the single- and two-photon processes.

Returning to the case in which the coupling field is not manually detuned, we conclude that the two-photon process in a Vee scheme is strong for the zero velocity atoms because the coupling field is on resonance and significantly populates level $|2\rangle$. Furthermore, when the coupling field is Doppler shifted from resonance the two-photon effect diminishes because significant population is no longer excited into level $|2\rangle$. Consequently, the two-photon absorption is present for atomic velocities close to zero for which the two routes to absorption interfere and we have EIT, and it is absent for higher-velocity atoms when it would otherwise overlap and mask the transparency at line center.

Due to the fortuitous nature of the two-photon process in a Vee scheme the transparency induced therein is better than in a cascade or Λ scheme for each of the wavelength regimes. Indeed, comparison of the transparency induced in the mismatched ($\lambda_c > \lambda_p$) Vee scheme and the matched ($\lambda_c = \lambda_p$) cascade and Λ systems indicates that while the transparency is slightly deeper in the latter case it is broader in the former. Direct comparison of the absorption profiles in the mismatched $\lambda_c > \lambda_p$ regime for all schemes shows that transparency is present in the Vee scheme while completely destroyed in the cascade and Λ systems, for our selected coupling field Rabi frequency. Figure 9 indicates the on-resonance absorption as a function of coupling field Rabi frequency. We can see that transparency is possible in the cascade and Λ schemes by employing a coupling field Rabi frequency large enough to split the overlapping Autler-Townes components away from line center by more than the Doppler width, as expected. However, importantly, transparency is achieved in the Vee scheme for a coupling field Rabi frequency significantly lower than the Doppler width (approximately 500 MHz).

## V. FURTHER THEORETICAL CONSIDERATIONS

The main results of the presented analysis have been discussed. We now consider some further points of interest that arise from the theoretical model. Firstly, in Figs. 3, 4, and 5 we see that as the coupling wavelength increases so does the range over which absorption may be observed in all three schemes. This increase in bandwidth occurs because the two-photon process persists for higher-velocity atoms due to the reduction in the magnitude of the Doppler shift for a given atomic velocity. There is a corresponding reduction in the peak-predicted absorption because the total number of ab-

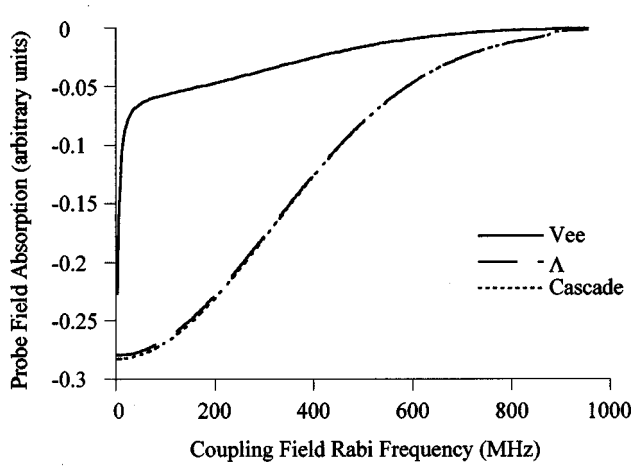


FIG. 9. The on-resonance transparency is plotted as a function of linear coupling field Rabi frequency for all three EIT schemes. The Vee-type scheme is depicted by a solid line and the cascade and Λ systems are indicated by dotted and dashed lines, respectively.

sorbing atoms remains constant. The total integrated absorption is always the same regardless of the choice of probe and coupling wavelengths.

Secondly, if we compare the magnitudes of the Autler-Townes components of the cascade and $\Lambda$ schemes we notice, for example, that while the absorption profiles for the matched wavelength systems are identical in Fig. 2 the Autler-Townes absorptions in Figs. 3 and 4 are of a lower magnitude in the $\Lambda$ scheme. This apparent discrepancy is due to linewidth effects. Referring back to Fig. 1, we see that for the Lambda scheme both the decay rates $\Gamma_{31}$ and $\Gamma_{32}$ describe population movement out of the upper level of the probe transition. The total decay from this level in the $\Lambda$ scheme, which determines the linewidth, is therefore twice the value for the cascade- and Vee-type systems. Consequently, the absorption profile of each individual Autler-Townes component is spread out in wavelength and reduced in peak magnitude, with no change in the total absorption. When we integrate over all atomic velocities, we therefore get the same ''net'' absorption profile in the cascade and $\Lambda$ schemes for the matched wavelength case.

Interestingly, if we consider the absorption profiles for the matched energy level schemes in Fig. 2 we see two sharp peaks on either side of line center. These are created because the two-photon resonance point is fixed for all velocities and the secondary Autler-Townes components line up with the zero velocity components to form sharp peaks of high magnitude on either side of resonance. In the Vee-type energy level scheme these peaks are of a significantly lower magnitude. This result is a consequence of the two-photon process diminishing rapidly when the coupling field is detuned.

So far, we have failed to take into account the effect of coupling field saturation. The cynic may claim that the difference in the three energy level schemes is a result of population transfer due to this effect rather than EIT. It is true to say that coupling field saturation plays its part in reducing the absorption as it does in any system based on a Vee scheme, but it is not the presence of this effect that allows us to observe transparency in the $\lambda_c > \lambda_p$ regime, rather the absence of it. Coupling field saturation occurs in a Vee scheme because the coupling field is connected to the ground state and, therefore, excites a fraction of the population from that state into the upper level of the coupling field transition. The exact proportion of the population excited in this way will depend upon the strength of the coupling field. There is, of course, an upper limit that occurs when the coupling field transition is saturated and the populations in the upper and lower levels are equalized. In a Doppler-broadened system this process is velocity selective. While the velocity group of atoms for which the coupling field is on resonance will quickly become saturated, other velocity groups for which the coupling field is detuned will not. In the latter case, the effects of coupling field saturation are minimal.

Coupling field saturation is inextricably linked to EIT since the latter effect relies on the interference of single- and two-photon absorption, and the magnitude of the two-photon absorption is dependent on the population in the upper level of the coupling transition. If we consider Figs. 3, 4, and 5 we see that the lack of a reduction in absorption in the cascade and $\Lambda$ schemes is not due to a lack of induced transparency for the zero velocity group at line center. In fact, EIT still takes place for atoms at rest, but it is masked by the secondary Autler-Townes absorptions of the higher-velocity groups. In the Vee scheme, we still observe the transparency that is induced at line center in the normal way, because the secondary Autler-Townes components—associated with the high-velocity groups—that overlap with line center are very small in magnitude. As discussed earlier, these Autler-Townes components are reduced in magnitude because the two-photon process is greatly diminished when the coupling field is detuned form resonance, i.e., when the coupling field saturation effect is negligible. It is, therefore, the lack of coupling field saturation for high-velocity atoms that allows us to observe transparency in the Vee-type scheme for probe frequencies higher than the coupling field frequency. It is, of course, the case that absorption is halved by coupling field saturation of the zero velocity group atoms, but EIT effects reduce absorption well beyond this limit.

## VI. EXTENDING THE WAVELENGTH MISMATCH

The results discussed in this paper can be broadly applied to any mismatched Doppler-broadened system. We have chosen to mismatch the wavelengths by varying the coupling field frequency while that of the probe is constant. In a real experimental scheme it would be more likely that the coupling field remained in the visible region of the spectrum while a higher frequency was sought on the probe transition. However, it is the case that the level of transparency achievable in a system is the same for the same ratios of both coupling field to probe field wavelengths and driving Rabi frequency to Doppler width, regardless of the actual wavelengths involved. One further caveat is that the transition decay rates will also effect the level of observed transparency.

For the Vee scheme we have seen that in the $\lambda_c > \lambda_p$ regime significant transparency is predicted for a driving frequency that is half the Doppler width. In this system, the ratio of coupling and probe wavelengths is 2:1. We can, therefore, expect that a 200-nm coupling transition driving a 100-nm probe transition will induce that same level of transparency if the coupling field Rabi frequency is adjusted to be half the new Doppler width and the transition decay rates are unchanged. If we further increase the ratio of coupling and probe fields then we would expect the induced transparency to degrade. In order to investigate this we have selected a Vee scheme in which the coupling field is visible (500 nm) and kept constant while the probe field wavelength is reduced; decay rates are the same as before. The ratios looked at are approximately 2:1, 4:1, 8:1, and 16:1 and the results are shown in Fig. 10. As the probe field is changed the coupling field strength is altered to maintain the coupling field Rabi frequency at half the probe field Doppler width in each case; if the Rabi frequency were not changed in this way we would expect the transparency to degrade more significantly. This takes the probe field down to 30 nm, well into the vacuum ultraviolet. As can be seen, once the ratio increases to 8:1 (the probe at 60 nm) there is no transparency window. There is, however, a reduction in absorption due to the presence of the coupling field beyond that expected from coupling field saturation alone. This reduction does manifest it-

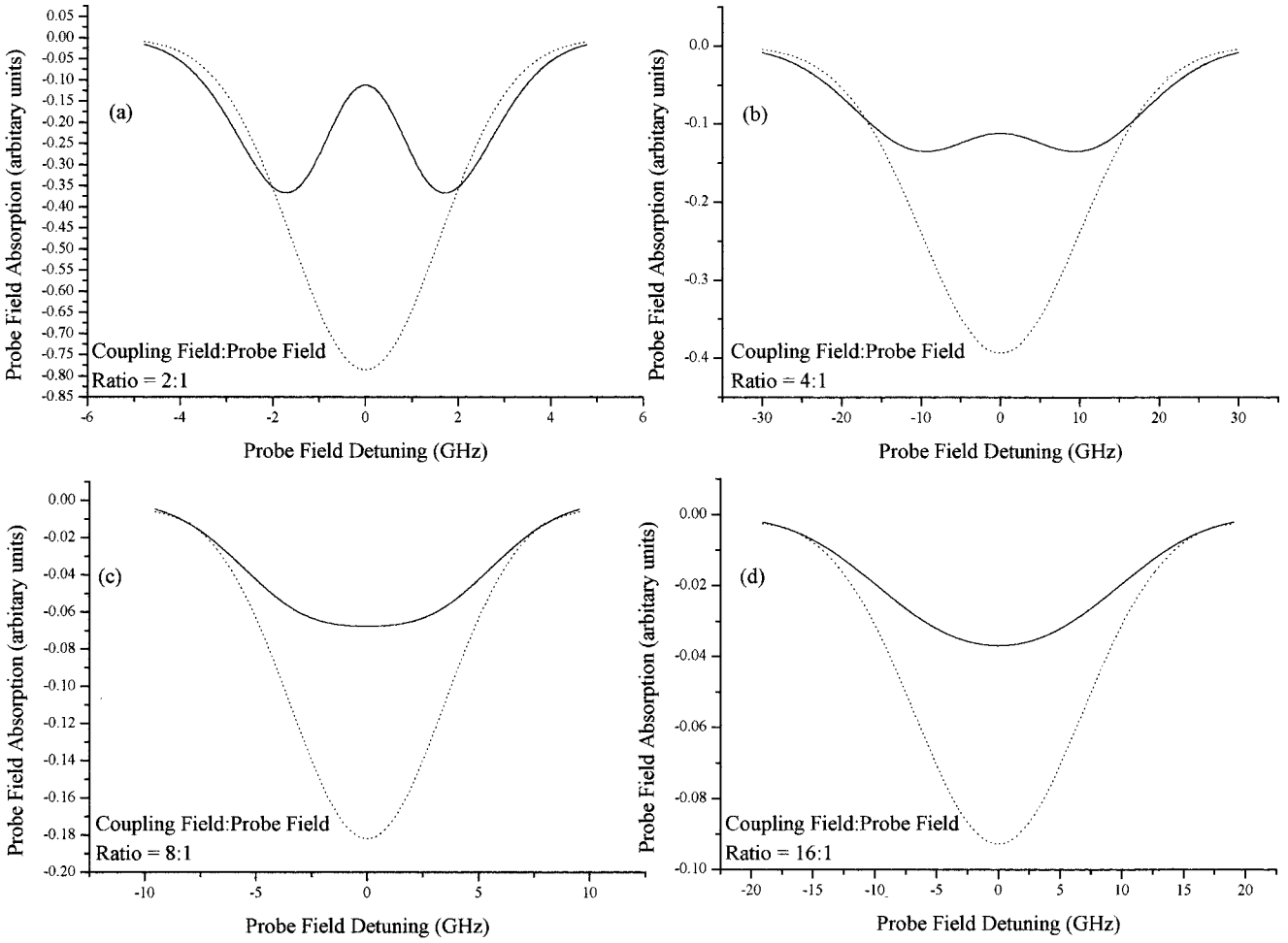


FIG. 10. Plots of probe field absorption as a function of probe field detuning in a mismatched Vee scheme. In all cases the coupling field is 500 nm. In (a) the probe field is 250 nm, (b) 125 nm, (c) 60 nm, (d) 30 nm. The transparency window is seen to degrade as the ratio of coupling field to probe field is increased.

self as an EIT window as the absorption reduction is spread out over the entire Doppler line-shape function.

The implication is that EIT can be induced, in cases where the Rabi splitting is half the Doppler width, for coupling field-probe field wavelength ratios of approximately 4:1 or less. In moving to higher ratios the Vee-scheme advantage is lost and Rabi splitting comparable or greater than the Doppler width is required. Such results are important when practical inversionless lasing systems are under consideration. They are also important in schemes where a radio frequency field acts as the coupling field [30], indicating that a large amount of power will be required to induce transparencies on an optical transition.

## VII. CONCLUSION

The result that EIT is strongest for the mismatched $\lambda_c < \lambda_p$ wavelength regime in a Cascade scheme has been demonstrated to apply to all three energy level configurations. We have also highlighted the robust nature of the Vee-type system that results from the unique form of the two-photon process. While the induced transparency is more pronounced when the coupling field frequency is higher than that of the probe, induced transparency is still realizable for high-frequency probe systems in a Vee-type scheme. Indeed, the transparency induced in the mismatched Vee configuration ($\lambda_c > \lambda_p$) compares favorably with that induced in the matched cascade and $\Lambda$ systems. While we have not employed a real atomic system in this analysis we have clearly shown that EIT can be realized in a probe field twice the frequency of the coupling field for a sub-Doppler width Rabi frequency. These results imply that the exploitation of quantum coherence effects are not confined to matched wavelength systems in Doppler-broadened media, and that the Vee scheme provides the best potential level of transparency in a system subject to Doppler effects, particularly for configurations in which the probe frequency is far in excess of the coupling field frequency. These results may also have wider implications for other inhomogeneously broadened media such as quantum wells.

## ACKNOWLEDGMENTS

This work was funded by the Engineering and Physical Sciences Research Council (EPSRC) under Grant No. GR/L32118. J. R. Boon, E. Zekou, and D. McGloin would also like to acknowledge EPSRC and St. Leonard's College for personal financial support.

[1] J. Gao *et al.*, Opt. Commun. **93**, 323 (1992).
[2] A. Nottleman, C. Peters, and W. Lange, Phys. Rev. Lett. **70**, 1783 (1993).
[3] W. E. van der Veer *et al.*, Phys. Rev. Lett. **70**, 3243 (1993).
[4] E. S. Fry *et al.*, Phys. Rev. Lett. **70**, 3235 (1993).
[5] J. A. Kleinfeld and A. D. Streater, Phys. Rev. A **49**, R4301 (1994).
[6] A. S. Zibrov *et al.*, Laser Phys. **5**, 553 (1995).
[7] Y. Zhu and J. Lin, Phys. Rev. A **53**, 1767 (1996).
[8] C. Fort *et al.*, Opt. Commun. **139**, 31 (1997).
[9] A. V. Durrant *et al.*, Opt. Commun. **151**, 136 (1998).
[10] A. S. Zibrov *et al.*, Phys. Rev. Lett. **75**, 1499 (1995).
[11] C. Peters and W. Lange, Appl. Phys. B: Lasers Opt. **62**, 221 (1996).
[12] G. G. Padmabandu *et al.*, Phys. Rev. Lett. **76**, 2053 (1996).
[13] P. B. Sellin *et al.*, Phys. Rev. A **54**, 2402 (1996).
[14] F. B. de Jong *et al.*, Phys. Rev. A **57**, 4869 (1998).
[15] M. D. Lukin *et al.*, Laser Phys. **6**, 436 (1996).
[16] S. E. Harris, Phys. Today **50**(8), 36 (1997).
[17] M. H. Dunn, in *Laser Sources and Applications*, Proceedings of the 47th Scottish Universities Summer School in Physics, St. Andrews, Scotland, 1995, edited by A. Miller and D. M. Finlayson (IOP, London, 1996).
[18] J. H. Marangos, J. Mod. Opt. **45**, 471 (1998).
[19] B. Lu, W. H. Burkett, and M. Xiao, Opt. Commun. **141**, 269 (1997).
[20] G. Vemuri and G. S. Argarwal, Phys. Rev. A **53**, 1060 (1996).
[21] S. Shepherd, D. J. Fulton, and M. H. Dunn, Phys. Rev. A **54**, 5394 (1996).
[22] J. R. Boon, E. Zekou, D. J. Fulton, and M. H. Dunn, Phys. Rev. A **57**, 1323 (1998).
[23] D. J. Fulton, S. Shepherd, R. R. Moseley, B. D. Sinclair, and M. H. Dunn, Phys. Rev. A **52**, 2302 (1995).
[24] J. Vanier, *Basic Theory of Lasers and Masers* (Gordon and Breach, London, 1971).
[25] R. R. Moseley *et al.*, Phys. Rev. A **50**, 4339 (1994).
[26] A. Imamoglu, J. E. Field, and S. E. Harris, Phys. Rev. Lett. **66**, 1154 (1991).
[27] Y. Li and M. Xiao, Phys. Rev. A **51**, R2703 (1995).
[28] C. H. Townes and A. L. Schawlow, *Microwave Spectroscopy* (McGraw-Hill, London, 1955), p. 282.
[29] R. Moseley and M. H. Dunn, Phys. World **8**, 30 (1995).
[30] S. F. Yelin *et al.*, Phys. Rev. A **57**, 3858 (1998).